Eur. Phys. J. Appl. Phys. **94**, 30301 (2021)

https://doi.org/10.1051/epjap/2021200365

THE EUROPEAN PHYSICAL JOURNAL APPLIED PHYSICS

Regular Article

Sustained coherent epitaxy and role of oxygen vacancies in $La_{0.7}Sr_{0.3}MnO_{3-\delta}$ thin films grown on $SrTiO_3$ by sputtering

Mohamed Lmouchter[1,*] and Minoru Suzuki[2]

[1] Department of Physics, Polydisciplinary Faculty of Ouarzazate, Ibn Zohr University, B.P. 638, Ouarzazate 45000, Morocco
[2] Department of Electronic Science and Engineering, Kyoto University, Kyoto 615-8510, Japan

Received: 28 November 2020 / Received in final form: 24 February 2021 / Accepted: 21 May 2021

Abstract. Ferromagnetic $La_{0.7}Sr_{0.3}MnO_{3-\delta}$ (LSMO) epitaxial thin films of single-crystal quality with very smooth surfaces are grown on $SrTiO_3$ (100) substrates by on-axis rf magnetron sputtering. We find that the resistivity and the spontaneous magnetization for these 180 nm thick films are nearly equal to those of single crystals after thermal annealing. On the other hand, the Curie temperature T_C is no higher than 270 K, a value far below the bulk one, which is quite unusual. As a clue to this riddle, we note a strong correlation between the lattice constant for these films and the amount of oxygen vacancies in the case of LSMO, an oxygen-nonstoichiometric oxide. From this, we conclude that the sustained coherent epitaxy takes place to match the lattice mismatch of 0.8% by incorporating a limited amount of oxygen vacancies, which relaxes the film in-plane stress while functions to significantly reduce T_C.

1 Introduction

The $La_{0.7}Sr_{0.3}MnO_{3-\delta}$ (LSMO) system is a perovskite-type ferromagnet with the highest Curie temperature T_C of 370 K at $\delta \sim 0$ [1]. The ferromagnetism of this material derives from the double exchange interaction [2,3], and hence the ferromagnetic transition is accompanied by a metal-insulator transition. At temperatures near the transition, LSMO exhibits a significantly large magnetoresistance, which has been attracting interest in its potential application to sensors [4] and other electronic devices [5–8]. In addition, perfect spin polarization associated with the double exchange interaction is also attractive for the spin-tunneling devices [5,6,8–10]. These features have been stimulating many researches into thin film preparation of this material.

Now, an increasing number of researchers into thin film preparation employ the pulsed-laser deposition method (PLD) [11,12], an effective method for the thin film growth of oxides and other complex compounds [5,7,13,14]. Indeed, this method has been quite successful in the growth of high-quality thin films for high-T_c cuprates [15].

On the other hand, the sputtering method, while effective for many purposes and for many materials, has a problem in the case of oxide film deposition. This problem is known as the resputtering effect [16,17], in which the substrate surface is bombarded by negative ions, mostly O^-, produced at the cathode surface. This effect results in a reduced deposition rate and an altered film composition. In an extreme case, no deposition is obtained. This drawback is, however, circumvented by a number of techniques, such as off-sputtering [18], off-center sputtering [19], or hollow cathode sputtering [20]. It can be circumvented also in on-axis sputtering, as the present study shows, providing complex oxide thin films of high crystal quality. However, there is an unclarified problem that a certain physical property, such as T_C, for these thin films is greatly suppressed compared with that of bulk single crystals.

In this paper, we report epitaxial growth of LSMO thin films on $SrTiO_3$ (100) single crystal substrates by on-axis rf magnetron sputtering under conditions suppressing the resputtering effect. The thin films grown at 820 °C are of crystal quality comparable with that of bulk single crystals with very smooth film surfaces despite the lattice mismatch of 0.8%. On the other hand, the value for T_C of ~270 K remained far below the bulk value even after thermal annealing in oxygen though the resistivity and the spontaneous magnetization were almost equal to the bulk values and the films are of high crystal quality. We interpret these unusual results in terms of a two-fold role played by the oxygen vacancies both in sustaining coherent epitaxy and in suppressing T_C. This behavior of oxygen vacancies in epitaxial growth is characteristic to oxygen-nonstoichiometric oxides like LSMO, where the oxygen content varies relatively freely depending on the oxygen partial pressure and the temperature the specimen experienced [21,22].

2 Experimental

2.1 Sputtering configuration and conditions

The rf sputtering equipment used by us employed a magnetron cathode 4 inch in diameter with concentric permanent magnets underneath. The inner circular magnet

* e-mail: m.lmouchter@uiz.ac.ma

was 35 mm in diameter and the outer ring magnet had 80 mm in inner diameter. Corresponding to these concentric magnets, a ring erosion area of approximately 4 and 8 cm in inner and outer diameters, respectively, was formed on the surface of the target.

The substrate was placed 4.5 cm directly above the center of the target so as not to confront the erosion area. The substrate was heated by radiation from a spirally wound Kanthal wire through transparent fused quartz. The surface of the Kanthal wire was thoroughly oxidized in air for about 1 day by passing an electrical current before use in vacuum. Thus a substrate temperature $T_{\rm sub}$ as high as 820 °C was attained.

The substrates used were $SrTiO_3$ (STO) (100) single crystals with a size of $10 \times 10 \times 0.5$ cm^3. The sputtering atmosphere was a mixed gas of 70% Ar and 30% O_2, and the sputtering pressure we finally adopted was 11 Pa. The rf power was fixed at 3 W/cm^2. After the growth, LSMO films were spontaneously cooled as they were either in vacuum or in 9.3×10^4 Pa O_2. The latter cooling process belongs to the so-called *in situ* annealing. Some of the grown films were annealed in a tubular furnace at 900 °C for 2 h in O_2 (post-annealing). The O_2 flowing rate was $1\,l$/min and the pressure was approximately 10^5 Pa.

2.2 Sputtering targets

For sputtering targets, appropriate mixtures of La_2O_3, $SrCO_3$, Mn_2O_3 of 99.9% purity were mixed and ground in an automated motar for 40 min and calcined in air at 1200 °C for 12 h. The reactants were pulverized, then ground and calcined again under the same conditions. This process was repeated two times. Then the powders were mixed with 4 wt% of 10 wt% polyvinyl alcohol water solution, ground for 20 min, and granulated by passing them through a sieve of 420 μm opening. The granular powders were pressed at about 2 MPa into a plate 110 mm in diameter and approximately 6 mm high using a mould, then rubber-pressed hydrostatically at 200 MPa, and finally sintered at 1500 °C for 20 h in flowing O_2. The targets thus obtained were La-Sr-Mn-O mixed complex compound oxides. The target composition finally adopted was [La]:[Sr]:[Mn] = 0.7:0.34:1.27, which was compensated for Sr and Mn.

2.3 Measurements

Film thicknesses were determined with a stylus profilometer at a step made by etching an LSMO film with a mixed acid of 40% HCl+40% HNO_3+20% H_2O. The deposition rate was 18 nm/min and the thickness of the LSMO films dealt with in this paper was 180 nm.

Film compositions for La, Sr, and Mn were estimated by energy-dispersive spectroscopy (EDS). X-ray diffraction (XRD) and reflection high-energy electron diffraction (RHEED) were used to characterize the surface structure and epitaxy for the grown films.

Magnetizations were measured with a SQUID magnetometer (MPMS, Quantum Design Inc.) under an applied magnetic field of 0.5 T parallel to the film surface. The contribution from the substrate was subtracted based on measurements done on a blank substrate. Electrical resistivities were measured by the four probe method in the temperature range from 10 K to 400 K on a 0.3×1.8 mm^2 linear strip made by chemical etching.

3 Results

3.1 Film compositions

The EDS analysis showed that the atomic ratios of [Sr]/[La] and [Mn]/[La] tend to decrease from the target values by approximately 10% and 20%, respectively. When the compensated target of [La]:[Sr]:[Mn]=0.7:0.34:1.27 was used, the film compositions became close to $La_{0.7}Sr_{0.3}MnO_{3-\delta}$. Fine composition adjustment was carried out by controlling the sputtering pressure so as to reduce to the minimum the amount of precipitates, which necessarily result on the film surface due to composition deviation from the cationic stoichiometry at high growth temperatures, as done in references [23,24]. No appreciable change in the cationic composition was observed when $T_{\rm sub}$ was varied within the range from 650 °C to 820 °C.

3.2 Epitaxial growth

Figure 1 shows a typical XRD pattern for an as-grown LSMO thin film grown at $T_{\rm sub}$ = 820 °C under the optimal condition mentioned above. The pattern exhibits only (l00) peaks, indicating the growth of the LSMO (100) plane. Moreover, the FWHM value of the (200) peak is 0.13° and the Kα_2 peak is clearly discernible, both of which show that the film is of high crystal quality.

Figure 2 shows an RHEED pattern for such an LSMO film. The streaky pattern implies that the film surface is very smooth in a large area of the order of a few mm at least, and the background halation in the RHEED photo is indicative of the Kikuchi pattern. These results show that the LSMO films have grown on STO (100) epitaxially and that the films are of crystal quality comparable with that of bulk single crystals, i.e., the number of defects such as dislocations are greatly reduced in these films. Almost no precipitates were observed on the film surface. When we take into consideration the streaky RHEED pattern and the high growth temperature of 820 °C, it is highly probable that the atomic migration on the surface is enhanced and the LSMO films were grown in the layer-by-layer mode as in the case of $PbTiO_3$ on STO [25].

3.3 Lattice constant

In the present study, the crystal structure of the LSMO films is regarded as pseudocubic, as is the case for thin films of nearly cubic materials. In the case of $La_{0.7}Sr_{0.3}MnO_3$, its crystal structure is rhombohedral with a tilting angle of 60.35° [26], very close to 60°, which suffices to give the basis to the above assertion.

The inset into Figure 1 shows a plot for the out-of-plane lattice constant as a function of $T_{\rm sub}$ for as-grown LSMO epitaxial films, showing that the lattice constant decreases with increasing $T_{\rm sub}$, being 3.91 Å for $T_{\rm sub}$ = 650 °C and 3.87 Å for 820 °C. Clearly, the lattice constant

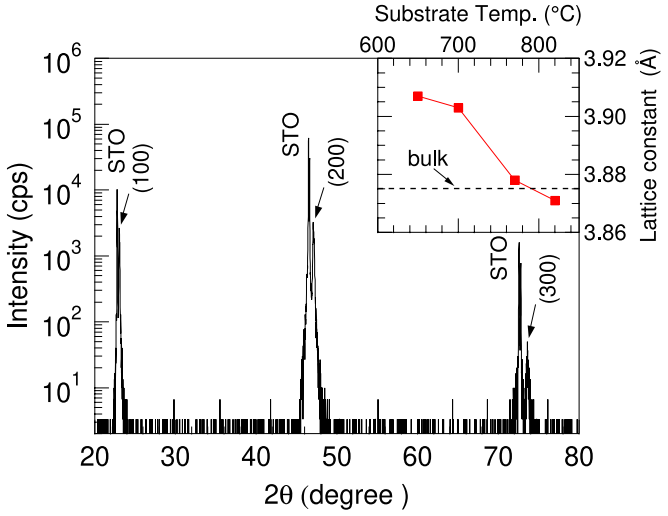

Fig. 1. A typical XRD pattern observed for an $La_{0.7}Sr_{0.3}MnO_{3-\delta}$ epitaxial thin film grown on STO (100) at 820 °C. The inset plots the lattice constant observed vs the substrate temperature.

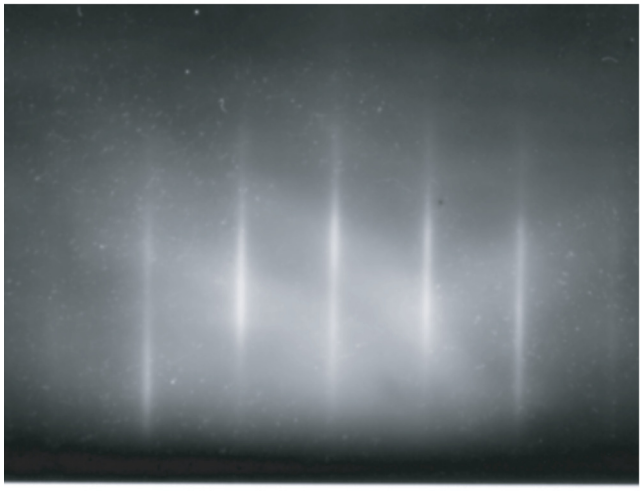

Fig. 2. A typical RHEED pattern observed for an $La_{0.7}Sr_{0.3}MnO_{3-\delta}$ epitaxial thin film grown on STO (100) at 820 °C.

is rather elongated when T_{sub} is less than ~800 °C. It should be also noted that the lattice constant for T_{sub} = 820 °C is a little smaller than the value of 3.875 Å for the bulk LSMO [26]. This may indicate that the ratio [Sr]/([La]+[Sr]) for the film is less than 0.3 [26]. Otherwise, it may indicate that the out-of-plane compressive strain remains associated with the in-plane tensile stress generated by the interface between the substrate and the epitaxial film. We discuss later, based on the transport and magnetic properties, that the lattice constant for the LSMO epitaxial films is strongly related to the existence of oxygen vacancies.

3.4 Transport and magnetic properties

Figure 3 shows the temperature T dependence of electrical resistivity ρ for the LSMO epitaxial films grown at

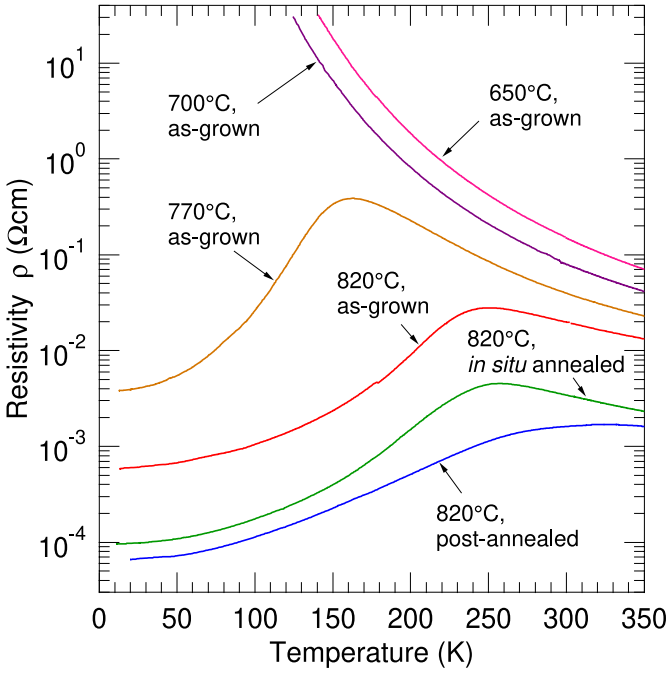

Fig. 3. Temperature dependence of electrical resistivity ($\rho - T$) for $La_{0.7}Sr_{0.3}MnO_{3-\delta}$ epitaxial thin films grown on STO (100): as-grown at T_{sub} = 650 °C, 700 °C, 770 °C, and 820 °C; post-annealed at 900 °C in 10^5 Pa O_2 for 2 h (T_{sub} = 820 °C), and *in situ* annealed in 9.3×10^4 Pa O_2 (T_{sub} = 820 °C).

various T_{sub} from 650 °C to 820 °C. As T_{sub} increases, the $\rho - T$ curve for the as-grown films changes from semiconductive to partially metallic behavior with a peak. The peak structure seen for $T_{sub} \geq 770$ °C indicates the metal-insulator transition which accompanies the ferromagnetic transition in LSMO. In combination with the inset into Figure 1, Figure 3 implies a strong correlation between the lattice constant and ρ. LSMO films grown at or lower than 770 °C are likely to be deficient in hole carriers (i.e. Mn^{4+} ions). Therefore, the elongation of the lattice constant is thought to be closely relevant to the deficiency of hole carriers, which comes from oxygen vacancies. Since the ferromagnetism of LSMO is based on the double exchange interaction, T_C has also a strong correlation with the lattice constant, as discussed in the following section.

Although ρ is metallic at low temperatures for the as-grown film of T_{sub} = 820 °C, its value of 6×10^{-4} Ωcm is still one order of magnitude larger than the value of 5×10^{-5} Ωcm for bulk single crystals [1]. This implies that the film has a reduced hole concentration, which is explained in terms of the existence of a considerable amount of oxygen vacancies. Indeed, as seen in Figure 3, when such films were annealed in flowing O_2 at 900 °C, ρ decreased to a value of 6×10^{-5} Ωcm, which is nearly equal to the bulk value, implying that the oxygen vacancies are mostly removed. In Figure 3, it is also noteworthy that when the epitaxially grown LSMO films were cooled *in situ* in 9.3×10^4 Pa O_2, ρ at 10 K decreased to 9×10^{-5} Ωcm. This implies that even the epitaxial films can release a good amount of oxygen atoms when they are cooled in vacuum. Namely, the as-grown LSMO films are

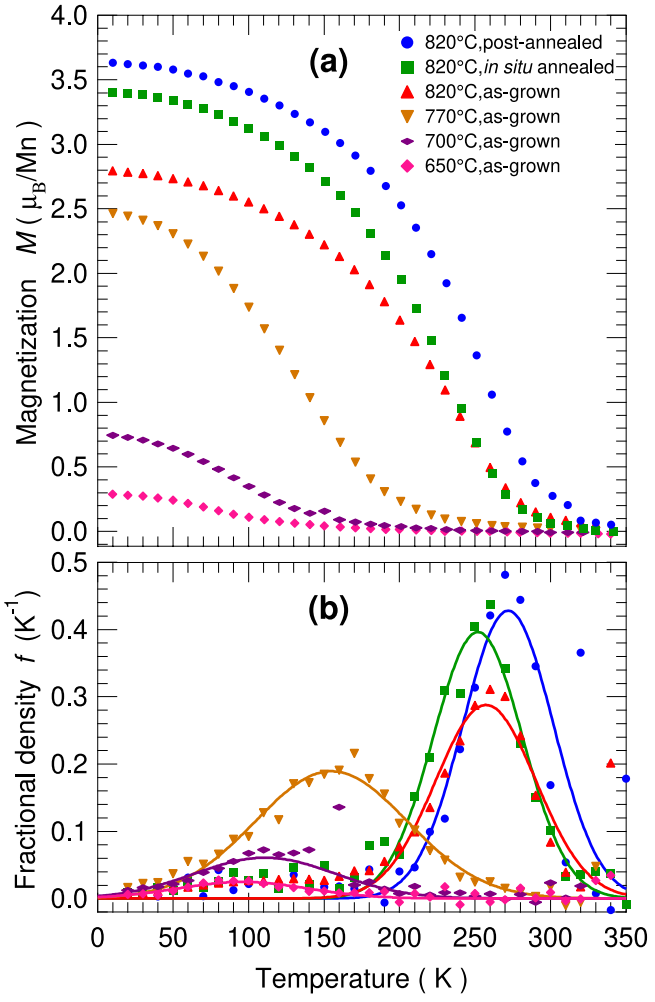

Fig. 4. (a) Temperature dependence of magnetization ($M-T$) for $La_{0.7}Sr_{0.3}MnO_{3-\delta}$ epitaxial thin films grown on STO (100): as-grown at T_{sub} = 650 °C, 700 °C, 770 °C, and 820 °C; post-annealed at 900 °C in 10^5 Pa O_2 for 2 h (T_{sub} = 820 °C), and *in situ* annealed in 9.3×10^4 Pa O_2 (T_{sub} = 820 °C). (b) Fractional density distribution f of T_C as calculated using the method described in the footnote of Section 3.4. The solid curves are least square fits using the normal distribution function, whose peak position has been adopted as T_C.

oxygen-deficient. Thus, it is thought that the LSMO epitaxial films in the present study contain a varying amount of oxygen vacancies, depending on T_{sub} and the treatment carried out after the growth. Therefore, the systematic change in ρ shown in Figure 3 is brought about as the amount of oxygen vacancies decreases systematically.

Figure 4a shows the T-dependence of magnetization M for the same epitaxial LSMO films shown in Figure 3. It is seen that all the as-grown LSMO films undergo a ferromagnetic transition, though no trace of the transition was seen in the $\rho-T$ curves for the LSMO films grown at a T_{sub} of 700 °C or lower. Therefore, it is likely that ferromagnetic regions exist as small isolated islands in these films.

For the films grown at a T_{sub} of 770 °C or 820 °C, a clear transition is seen in $M-T$. However, the transitions are rather broad, suggesting that the films consist of regions of distributed T_C. In order to evaluate the representative T_C value for the most of regions, we have derived the fractional density distribution f as a function of T_C based on the mean field theory,[1] as shown in Figure 4b, where peak positions are adopted as the values for T_C. For the as-grown films, T_C increases from ~100 K to ~260 K as T_{sub} increases from 650 °C to 820 °C, and at the same time, M(10 K) increases from 0.3 to 2.8 μ_B/Mn. A comparison between the behaviors of $\rho-T$ in Figure 3 and $M-T$ in Figure 4a suggests that, as T_{sub} increases, ferromagnetic, i.e., metallic, islands nucleate, then their sizes increase, and finally connect totally with others, forming a structure like stripes. Therefore, the present experimental result is consistent with the inhomogeneous model envisaged for underdoped manganates [27] and cuprates [28].

The effects of post- and *in situ* annealing on the T-dependences of ρ and M are also shown in Figure 3 and Figure 4a, respectively. By post-annealing at 900 °C, the peak position of the $\rho-T$ curve shifted toward higher temperatures and ρ(10 K) decreased by almost one order of magnitude to a value of 6×10^{-5} Ωcm, which is almost equal to the bulk value of 5×10^{-5} Ωcm [1]. By *in situ* annealing, on the other hand, it turned out that ρ decreased by a factor of 0.17 while its peak position remained at nearly the same temperature. From this result, it is presumed that oxygen atoms were released inhomogeneously while the films were being cooled in vacuum after the growth, and that it occurred preferentially in the regions neighboring the oxygen-deficient ones. Therefore, T_C remained almost unchanged in a part of the film, while ρ increased by almost one order of magnitude in the other part where oxygen atoms were removed. This may imply, as an extreme inhomogeneous case, that oxygen-deficient LSMO films are composed of small ferromagnetic islands with less oxygen vacancies and other surrounding regions with more oxygen vacancies. It is also probable that this inhomogeneity is accompanied by the presence of oxygen vacancy clusters proposed in rare-earth perovskite-type oxides [29].

It is also seen in Figure 4a that the value for M at low temperatures increased to 3.63 μ_B/Mn after post-annealing, a value close to the bulk value 3.7 μ_B/Mn. However, T_C increased only slightly from 260 to ~270 K, a value far below that of the bulk. The reason for this is suggested in the following section.

4 Discussion

4.1 Film growth in on-axis sputtering

From the present results, it follows that the resputtering effect can be mitigated to a large extent both by sputtering under a moderately high pressure of 11 Pa and

[1] Let $m(T,T_C)$ be the spontaneous magnetization at T for a ferromagnet with a transition temperature T_C in the mean field model, $f(T_C)$ the fractional distribution of T_C, $M(T)$ the T dependence of magnetization. Then $M(T)=\int m(T,T_C)f(T_C)\mathrm{d}T_C$ holds. $f(T_C)$ can be obtained by solving this integral equation numerically.

by placing a substrate in an area apart from the part confronting the target erosion area. Because such a high pressure as above increases the scattering rate of the sputtered atoms, composition deviation inevitably results from the difference between the scattering angles of heavier La and those of lighter Sr or Mn. It also causes a radial distribution of the thickness and the composition outside the circular central area of 2 to 3 cm in diameter [30]. In this circular area, the composition is nearly uniform, and it is in this area that we placed the substrate.

Since the lighter Mn and Sr atoms are scattered at larger angles than La, the Mn and Sr contents tend to be deficient in the LSMO films when sputtered under such conditions as above. Therefore, we compensated the target with Mn and Sr in order to obtain the cationic stoichiometry in the film composition. In this way, we were able to attain epitaxial growth of LSMO films by on-axis sputtering.

It should be also noted that the deposition rate of 18 nm/min in the present sputtering experiments is rather large when compared with that of PLD or off-axis sputtering. According to Gavaler et al. [18], the oxide film in the sputtering process is primarily oxygenated by radical oxygen produced at the target surface. If this is the case, radical oxygen is less sufficiently provided at a high growth rate, since the collision rate for the radical oxygen atoms increases.[2] Then, such a high growth rate as above may cause an increase in oxygen deficiency.

4.2 Lattice constant, oxygen vacancies, and sustained epitaxy

The inset into Figure 1 shows that when T_{sub} is below 700 °C, the out-of-plane lattice constant of the LSMO epitaxial films is nearly equal to that of STO, 3.905 Å, which is larger by 0.8% than the LSMO bulk value. It becomes close to the bulk value only when T_{sub} is higher than ~800 °C. Since a T_{sub} of ~700 °C is thought to be sufficiently high for the deposited atoms to be thermalized and migrate on the film surface to form the LSMO crystal structure at the thermal equilibrium, it is interesting to know why the lattice constant is so larger than the bulk value even when the thickness is as large as 180 nm.

It is naturally thought that STO is a suitable substrate material for the epitaxial growth of LSMO thin films, because STO and LSMO are of the same perovskite crystal structure with similar elements at corresponding cation sites. This gives rise to a strong interface affinity between the LSMO epitaxial film and the STO substrate. As a result, the LSMO film grows epitaxially and coherently[3] in spite of a mismatch of 0.8% under tensile strain with the in-plane lattice constant elongated to that of STO. However, this occurs only at the initial stage of the epitaxial growth when the film is very thin, say, 10 nm thick or so.[4]

The critical thickness, above which the influence of the interface diminishes, is usually thought to be much smaller than 180 nm even in the case of LSMO [32] as long as only the interface affinity and the in-plane compressive stress are concerned. This is because the in-plane compressive stress, normally existent in the film crystal structure, becomes dominant over the tensile stress exerted by the interface when the film thickness becomes several tens of times the lattice constant. Then, it is quite interesting to know the reason why the elongated lattice remains unrelieved when the thickness becomes as large as 180 nm or even larger.[5]

One probable solution to this puzzle is the role of oxygen vacancies introduced into the film during the epitaxial growth. Since LSMO is a kind of oxygen-nonstoichiometric complex compounds [22], as is the case for $YBa_2Cu_3O_{7-\delta}$ [34], it can incorporate a varying amount of oxygen vacancies. When an oxygen ion is absent at an oxygen site, the repulsive force increases among the cations around that site, which works to relieve the compressive stress partially and retain the lattice elongation. This is typically the case for the $YBa_2Cu_3O_{7-\delta}$ system, where the unit cell volume increases with the oxygen vacancy content [35]. It is this mechanism that gives rise to a scenario in which oxygen vacancies are properly introduced into the growing film so that the LSMO lattice constant is close to that of STO. If this happens, the coherent epitaxial growth of the LSMO film is sustained even after the initial stage, yielding films with an elongated in-plane lattice constant up to a film thickness greater than 180 or even 300 nm.

When T_{sub} is ~800 °C or higher, the out-of-plane lattice constant is nearly equal to the bulk value, as seen in the inset into Figure 1. This can be possible if oxygen vacancies in the LSMO epitaxial films are located so as to reduce the in-plane compressive stress but not the out-of-plane stress.[6] Accordingly, we presume that the LSMO epitaxial films grown at 820 °C contain a certain amount of oxygen vacancies even though the out-of-plane lattice constant is nearly equal to the bulk value.

4.3 Effect of thermal annealing

By post-annealing, $\rho(10\ K)$ and $M(10\ K)$ became nearly equal to the corresponding values for bulk LSMO [26], while T_C increased only marginally from ~260 K to ~270 K, which is far below the bulk value of 370 K. This implies that the post-annealing does not simply lead to the thermal equilibrium in the case of LSMO epitaxial films grown on STO.

For the reason of this significant reduction in T_C, we can name the tensile strain effect, Sr composition deviation, or the oxygen vacancy effect. For the first effect, even

[2] As the growth rate increases, the atomic fluence increases and the number of collisions between radical oxygen atoms and other sputtered atoms increases, reducing the arrival rate for lighter oxygen atoms.

[3] By 'coherently' we mean that the in-plane lattice constants are the same and dislocations are absent.

[4] In the case of YBaCuO films grown on MgO, for example, the strain in the YBCO film is relieved when the thickness increases beyond approximately 10 nm by incorporating cracks in the film, resulting in cube-packed surface morphology [31].

[5] Associated with the present result, it is noted that in the case of $La_{1.85}Sr_{0.15}CuO_4$ superconducting epitaxial films grown on STO, the critical thicknesses are 700 nm on (100) and 500 nm on (110) [33], which are much larger than the thicknesses in the present case.

[6] This can take place if oxygen atoms are removed selectively from the MnO_2 planes parallel to the film surface.

if it remains as much as in the case of 20 nm-thin epitaxial LSMO films, T_C would not decrease to lower than 330 K [32]. Therefore, solely the tensile strain effect is not sufficient to explain the result. The effect of deviation in Sr composition is also limited, because the decrease in T_C is estimated to be no larger than 20 K if the phase diagram for LSMO is consulted [26]. Therefore, the oxygen vacancy effect is the most probable cause of this significant reduction in T_C.

When one oxygen is removed from LSMO, two electrons are left behind, eliminating two holes. Thus, the oxygen vacancies reduce the number of Mn^{4+} ions. Furthermore, the removal of oxygen ions from the oxygen sites eliminates the double exchange interaction between Mn^{3+} and Mn^{4+} ions. Within the framework of the mean-field theory [36], T_C is roughly proportional to the product of the number of Mn^{4+} and the average exchange interaction energy for the chain of Mn^{3+}– O^{2-}– Mn^{4+}. In this respect, it follows that oxygen vacancies reduce T_C more pronouncedly than the conductivity and the spontaneous magnetization.

Next, the elongation of the in-plane lattice constant due to the oxygen vacancies is also responsible for the reduction in T_C. According to the theory by Anderson and Hasegawa [3], the exchange interaction energy reduces with the decrease in the transfer integral between d electrons at Mn sites. Clearly, the transfer integral decreases exponentially with the increase in the distance between Mn sites. Therefore, T_C decreases further with the oxygen vacancies also in this respect.

Thus a certain amount of oxygen vacancies still remains even after the post-annealing, reducing T_C pronouncedly. However, its density is limited because ρ at low T is as small as that of a single crystal. Since oxygen vacancies in the MnO_2 planes parallel to the surface function to reduce the in-plane compressive stress and to sustain coherent epitaxy, the present experimental results imply that the in-plane lattice elongation, rather than the tensile strain, sets in very stably in the LSMO epitaxial films when the oxygen vacancies are introduced by a proper amount into the epitaxial films.

It is worth mentioning the reason why ρ and M at low T are similar to those for the bulk single crystals despite the much lower T_C for the post-annealed LSMO film. It appears that $M(T)$ would increase with the oxygen vacancies since the number of $Mn^{3+}(2\mu_B)$ increases while that of $Mn^{4+}(1.5\mu_B)$ decreases. However, it is not necessarily the case and $M(T)$ decreases gradually with the increase in the density of oxygen vacancies for the reason which follows. The spontaneous magnetization is determined by the number of spin-aligned Mn^{4+} and Mn^{3+} ions in the region where holes are itinerant. In regions near oxygen vacancies, holes are absent because an oxygen vacancy interrupts the hole transport and further it plays effectively a role of $+2e$ charge, all of which reduce the double exchange interaction. Therefore, the increase in the hole-absent area due to oxygen vacancies causes rather a gradual decrease in $M(T)$, which is reflected on the present result.

As for ρ at low T, we should take into account the inhomogeneous distribution of oxygen vacancies as mentioned above. Because of this inhomogeneity, electrical current flows predominantly in the highly conductive regions, where oxygen vacancies are scarce. Therefore, no large increase in ρ obtains as long as the oxygen vacancy concentration is limited.

Finally, it is also worthy of mentioning that in order to relax the whole lattice strain and to remove the oxygen vacancies almost completely, it is necessary to introduce crystal defects like edge dislocation arrays or even microcracks. Another means is to introduce a buffer layer, which functions to relieve effectively the tensile strain as in the case of the high-T_c superconductor $YBa_2Cu_3O_{7-\delta}$ [31], or to use a substrate material with a much less lattice mismatch like $NdGaO_3$ or $LaSrAlO_4$ [32] with the aid of artificial radical oxygen source.

5 Conclusions

We have grown LSMO epitaxial thin films of single-crystal quality with very smooth surfaces on STO (100) substrates despite the lattice mismatch of 0.8%. The films, 180 nm thick, thus grown have the resistivity and the spontaneous magnetization nearly equal to those of bulk single crystals after annealing under 10^5 Pa O_2, while T_C is no higher than 270 K, falling far below the bulk value. These apparently unusual results are consistently interpreted in terms of the sustained coherent epitaxy in the presence of a limited amount of oxygen vacancies, which relaxes the film in-plane compressive stress while functions to significantly reduce T_C.

The authors would like to express their gratitude to Prof. S. Nishino at Kyoto Institute of Technology for the RHEED measurements. This work was supported in part by the Mitsubishi foundation.

Author contribution statement

M.L. planned and performed the experiments; M.S. supervised the work; all the authors processed the experimental data, performed the analysis, drafted the manuscript, and designed the figures; all the authors contributed to the final manuscript.

References

1. Y. Tokura, ed., *Colossal Magnetoresistive Oxides* (Gordon and Breach Science Publishers, 2000)
2. C. Zener, Phys. Rev. **82**, 403 (1951)
3. P.W. Anderson, H. Hasegawa, Phys. Rev. **100**, 675 (1955)
4. O. Rousseau, S. Flament, B. Guillet, M.L.C. Sing, L. Méchin, Proceedings **1**, 635 (2017)
5. S. Majumdar, S. van Dijken, J. Phys. D **47**, 034010 (2013)
6. M. Gajek, M. Bibes, M. Varela, J. Fontcuberta, G. Herranz, S. Fusil, K. Bouzehouane, A. Barthélémy, A. Fert, J. Appl. Phys. **99**, 08E504 (2006)
7. W. Pan, P. Lu, J.F. Ihlefeld, S.R. Lee, E.S. Choi, Y. Jiang, Q.X. Jia, Phys. Rev. Mater. **2**, 021401 (2018)

8. M. Bowen, M. Bibes, A. Barthélémy, J.P. Contour, A. Anane, Y. Lemaître, A. Fert, Appl. Phys. Lett. **82**, 233 (2003)
9. J.Y.T. Wei, N.C. Yeh, R.P. Vasquez, Phys. Rev. Lett. **79**, 5150 (1997)
10. J.H. Park, E. Vescovo, H.J. Kim, C. Kwon, R. Ramesh, T. Venkatesan, Nature **392**, 794 (1998)
11. D. Dijkkamp, T. Venkatesan, X.D. Wu, S.A. Shaheen, N. Jisrawi, Y.H. Min-Lee, W.L. McLean, M. Croft, Appl. Phys. Lett. **51**, 619 (1987)
12. T. Venkatesan, J. Phys. D **47**, 034001 (2013)
13. K. Dörr, K.H. Müller, E.S. Vlakhov, R.A. Chakalov, R.I. Chakalova, K.A. Nenkov, A. Handstein, B. Holzapfel, L. Schultz, J. Appl. Phys. **83**, 7079 (1998)
14. H. Hiramatsu, T. Katase, T. Kamiya, M. Hirano, H. Hosono, Appl. Phys. Lett. **93**, 162504 (2008)
15. M. Mukaida, S. Miyazawa, M. Sasaura, K. Kuroda, Jpn. J. Appl. Phys. **29**, L936 (1990)
16. S.M. Rossnagel, J.J. Cuomo, AIP Conf. Proc. **165**, 106 (1988)
17. J.J. Cuomo, R.J. Gambino, J.M.E. Harper, J.D. Kuptsis, J.C. Webber, J. Vac. Sci. Technol. **15**, 281 (1978)
18. J.R. Gavaler, J. Talvacchio, T.T. Braggins, M.G. Forrester, J. Greggi, J. Appl. Phys. **70**, 4383 (1991)
19. H. Asano, M. Asahi, O. Michikami, Jpn. J. Appl. Phys. **28**, L981 (1989)
20. X.X. Xi, G. Linker, O. Meyer, E. Nold, B. Obst, F. Ratzel, R. Smithey, B. Strehlau, F. Weschenfelder, J. Geerk, Z. Phys. B: Condens. Matter **74**, 13 (1989)
21. N. Abdelmoula, K. Guidara, A. Cheikh-Rouhou, E. Dhahri, J.C. Joubert, J. Solid State Chem. **151**, 139 (2000)
22. H. Tagawa, N. Mori, H. Takai, Y. Yonemura, H. Minamiue, H. Inaba, J. Mizusaki, T. Hashimoto, ECS Proc. Vol. **1997-40**, 785 (1997)
23. M. Naito, H. Sato, Appl. Phys. Lett. **67**, 2557 (1995)
24. H. Sato, A. Tsukada, M. Naito, A. Matsuda, Phys. Rev. B **61**, 12447 (2000)
25. K. Wasa, T. Satoh, H. Adachi, K. Setsune, Integr. Ferroelectr. **12**, 93 (1996)
26. A. Urushibara, Y. Moritomo, T. Arima, A. Asamitsu, G. Kido, Y. Tokura, Phys. Rev. B **51**, 14103 (1995)
27. E. Dagotto, New J. Phys. **7**, 67 (2005)
28. S. Kivelson, I. Bindloss, E. Fradkin, V. Oganesyan, J. Tranquada, A. Kapitulnik, C. Howald, Rev. Mod. Phys. **75**, 1201 (2003)
29. J.A.M. Van Roosmalen, E.H.P. Cordfunke, J. Solid State Chem. **93**, 212 (1991)
30. M. Suzuki, T. Murakami, Jpn. J. Appl. Phys. **22**, 1794 (1983)
31. K. Tsuru, S. Karimoto, S. Kubo, M. Suzuki, Jpn. J. Appl. Phys. **35**, L1666 (1996)
32. F. Tsui, M.C. Smoak, T.K. Nath, C.B. Eom, Appl. Phys. Lett. **76**, 2421 (2000)
33. H.L. Kao, J. Kwo, R.M. Fleming, M. Hong, J.P. Mannaerts, Appl. Phys. Lett. **59**, 2748 (1991)
34. K. Kishio, J. Shimoyama, T. Hasegawa, K. Kitazawa, K. Fueki, Jpn. J. Appl. Phys. **26**, L1228 (1987)
35. A. Manthiram, J.S. Swinnea, Z.T. Sui, H. Steinfink, J.B. Goodenough, J. Am. Chem. Soc. **109**, 6667 (1987)
36. N.W. Ashcroft, N.D. Mermin, *Solid State Physics* (Saunders College, 1976)

Cite this article as: Mohamed Lmouchter, Minoru Suzuki, Sustained coherent epitaxy and role of oxygen vacancies in $La_{0.7}Sr_{0.3}MnO_{3-\delta}$ thin films grown on $SrTiO_3$ by sputtering, Eur. Phys. J. Appl. Phys. **94**, 30301 (2021)